



**HAL**  
open science

## Trains of African Easterly Waves and Their Relationship to Tropical Cyclone Genesis in the Eastern Atlantic

Abdou Dieng, Laurence Eymard, Marion Leduc-Leballeur, Alban Lazar

### ► To cite this version:

Abdou Dieng, Laurence Eymard, Marion Leduc-Leballeur, Alban Lazar. Trains of African Easterly Waves and Their Relationship to Tropical Cyclone Genesis in the Eastern Atlantic. *Monthly Weather Review*, 2017, 145 (2), pp.599 - 616. 10.1175/mwr-d-15-0277.1 . hal-01833346

**HAL Id: hal-01833346**

**<https://hal.science/hal-01833346>**

Submitted on 12 Apr 2021

**HAL** is a multi-disciplinary open access archive for the deposit and dissemination of scientific research documents, whether they are published or not. The documents may come from teaching and research institutions in France or abroad, or from public or private research centers.

L'archive ouverte pluridisciplinaire **HAL**, est destinée au dépôt et à la diffusion de documents scientifiques de niveau recherche, publiés ou non, émanant des établissements d'enseignement et de recherche français ou étrangers, des laboratoires publics ou privés.

# Trains of African Easterly Waves and Their Relationship to Tropical Cyclone Genesis in the Eastern Atlantic

ABDOU L. DIENG AND SAIDOU M. SALL

*Laboratoire de Physique de l'Atmosphère et de l'Océan Siméon Fongang, Cheikh Anta Diop University, Dakar, Senegal*

LAURENCE EYMARD

*Laboratoire d'Océanographie et du Climat: Expérimentations et Approches Numériques, Pierre et Marie Curie University, Paris, France*

MARION LEDUC-LEBALLEUR

*Laboratoire de Glaciologie et Géophysique de l'Environnement, Grenoble, France*

ALBAN LAZAR

*Laboratoire d'Océanographie et du Climat: Expérimentations et Approches Numériques, Pierre et Marie Curie University, Paris, France*

(Manuscript received 11 August 2015, in final form 9 August 2016)

## ABSTRACT

In this study, the relationship between trains of African easterly waves (AEWs) and downstream tropical cyclogenesis is studied. Based on 19 summer seasons (July–September from 1990 to 2008) of ERA-Interim reanalysis fields and brightness temperature from the Cloud User Archive, the signature of AEW troughs and embedded convection are tracked from the West African coast to the central Atlantic. The tracked systems are separated into four groups: (i) systems originating from the north zone of the midtropospheric African easterly jet (AEJ), (ii) those coming from the south part of AEJ, (iii) systems that are associated with a downstream trough located around 2000 km westward (termed DUO systems), and (iv) those that are not associated with such a close downstream trough (termed SOLO systems).

By monitoring the embedded 700-hPa-filtered relative vorticity and 850-hPa wind convergence anomaly associated with these families along their trajectories, it is shown that the DUO generally have stronger dynamical structure and statistically have a longer lifetime than the SOLO ones. It is suggested that the differences between them may be due to the presence of the previous intense downstream trough in DUO cases, enhancing the low-level convergence behind them. Moreover, a study of the relationship between system trajectories and tropical depressions occurring between the West African coast and 40°W showed that 90% of tropical depressions are identifiable from the West African coast in tracked systems, mostly in the DUO cases originating from the south zone of the AEJ.

## 1. Introduction

African easterly waves (AEWs) are synoptic-scale disturbances observed between the surface and mid-troposphere from East (Sudan, Central African Republic, Chad) to West Africa (Niger, Nigeria, Burkina Faso, Mali) up to the Senegalese and Guinea coasts. They are the dominant synoptic weather systems in

West Africa and the tropical Atlantic during boreal summer and modulate rainfall in West Africa in relation with the mesoscale convective systems (MCSs) (Reed et al. 1977; Fink and Reiner 2003; Kiladis et al. 2006). They have a 3–5-day period and a mean wavelength of 2500 km and develop along two axes north and south of the AEJ. The north wave primarily grows in association with dry baroclinic energy conversions at the southern margin of the Sahara, while southern-track AEWs mainly result from barotropic instability and interaction with deep convection (Burpee 1972; Thorncroft and Hoskins

---

*Corresponding author e-mail:* Abdou Lahat Dieng, [abdoulahat.dieng@ucad.edu.sn](mailto:abdoulahat.dieng@ucad.edu.sn)

1994; Thorncroft and Blackburn 1999; Pytharoulis and Thorncroft 1999; Diedhiou et al. 1999). The southern vorticity is also a favored region for MCSs (Hodges and Thorncroft 1997), which can produce mesoscale vorticity anomalies. The north and the south tracks merge in the Atlantic, especially in the main development region (MDR) (see Goldenberg and Shapiro 1996; Goldenberg et al. 2001; DeMaria et al. 2001; Camara et al. 2011).

AEWs are known as the main precursors of tropical cyclones in the Atlantic (Pasch et al. 1998). It is estimated that they account for 60% of the Atlantic basin tropical storms and nonmajor hurricanes, and that they account for about 85% of major hurricanes (Landsea 1993). However, the proportion that strengthens to tropical cyclones among those leaving the West Africa coast is quite small [about 6%, see Hopsch et al. (2010) and Arnault and Roux (2011)]. Based on automatic tracking of vorticity centers in European Centre for Medium-Range Weather Forecasts (ECMWF) analyses, Thorncroft and Hodges (2001) developed a 20-yr climatology of African easterly wave activity and noted a marked interannual variability in AEW activity, especially at the 850-hPa level at the West African coast between about 10° and 15°N. They also found a notable positive correlation between this AEW activity and Atlantic tropical cyclone activity over the period between 1994 and 1998. Hopsch et al. (2007) extended the Thorncroft and Hodges (2001) analysis for 45 years using the ERA-40. Although they noted a positive correlation between the number of AEWs leaving the West African coast and the number of MDR tropical cyclones at seasonal and decadal time scales, they did not find any significant correlation at the interannual scale. Their study also revealed that most of the storms that reach the MDR are driven by the southern AEJ track while storms in the north track often dissipate very shortly after leaving the West African coast. Using a manual backtracking approach to identify the approximate genesis locations of AEWs transformed into tropical cyclones in the tropical Atlantic, Chen et al. (2008) found, contrary to Hopsch et al. (2007), that the tropical cyclones formed from AEWs that originate along the northern flanks of the AEJ (AEW<sub>n,s</sub>) are larger than those originated on the south (AEW<sub>s,s</sub>). Moreover they found that AEW<sub>n,s</sub> generally take long time to transform into tropical cyclones because they are drier and shallower. Using 33 years of ECMWF interim reanalysis (ERA-Interim) in the months of August and September, Chen and Liu, 2014 found that more than half of the low-level, moist vortices originating from south of the African easterly jet (AEJ) merged with a shallow, dry vortex from the north after leaving the West African coast and showed that this process occurred in the “predepression” stage of 70% of tropical cyclones (TCs) that formed in the MDR.

Additionally, observational and modeling case studies showed that the coupling between AEW and convective activity is essential for the tropical cyclone genesis in the eastern Atlantic Ocean. In particular, the tropical cyclone genesis is observed when MCSs are embedded in the trough region of the AEW (Berry and Thorncroft 2005; Hopsch et al. 2010; Camara et al. 2011; Arnault and Roux 2009, 2010, 2011; Chiao and Jenkins 2010; Leppert et al. 2013). Based on a nonhydrostatic model, Arnault and Roux, (2009) showed that the transformation of the AEW trough to the Tropical Storm Helene in August 2006 near Cape Verde resulted from a geostrophic adjustment following pressure decrease by embedded convection. More recently, Berry and Thorncroft (2012) examined the dynamical role of convection in AEW life cycles by using the Weather Research and Forecasting (WRF) Model in a single case from September 2004. Their sensitivity tests of such AEW to embedded convection showed that convection is vital for the maintenance of the AEW as it propagates across West Africa.

Under some underexplored conditions AEWs troughs that cross the tropical Atlantic in series can simultaneously strengthen (Peng et al. 2006; Vizy and Cook 2009; Diaz and Aiyyer 2013a,b; Dieng et al. 2014). Peng et al. (2006) observed that a unique train of easterly wave was responsible for the simultaneous genesis of Tropical Cyclones Danielle and Earl (both in 2004), located one wavelength apart, on 14 August 2004 in the Atlantic. They suggested that the formation of these two cyclones may have occurred through the intensification and scale contraction of the easterly waves. Vizy and Cook (2009) observed that the formation of Tropical Depression Debby (August 2006) over the Cape Verde region was preceded by a wave associated with the genesis of the depression associated with TC Ernesto in the western Atlantic. They argued that the passage of the AEW that later developed into Ernesto was a factor that preconditioned the lower troposphere, making the environment favorable for the development of the Debby wave by enhancing low-level southwesterly flow, convergence, horizontal low-level zonal shear, and cyclonic relative vorticity ahead of Debby. The AEW (which was further associated with the tropical depression pre-Ernesto) was downstream, approximately 2000 km to the west, of the Debby vortex. Based on observational satellite infrared brightness temperature and meteorological radar data over seven summer seasons between 1993 and 2006, Dieng et al. (2014) analyzed the structures of strengthening and dissipating MCSs evolving near the West African coast by subjectively selecting 20 cases of strengthening and dissipating MCSs in the vicinity of the Senegal coast. Their analyses confirmed that tropical cyclogenesis in the

eastern Atlantic is favored by an intense AEW trough downstream (e.g., Vizy and Cook 2009). Although Dieng et al. (2014) results are statistically significant; a limitation of their study is that the number of their case studies was relatively limited. In addition, their analyses were only based on subjective criteria and thus lead us to ask the following questions:

Is the presence of a previous trough of AEW a condition for the strengthened systems near the West African coast?

What is the relationship between the presence or absence of a previous AEW trough and tropical cyclogenesis off the West African coast?

The objective of this present study is to provide elements to respond to these questions. The first question is addressed through automatic tracking of successive AEW troughs and/or embedded MCSs in the tropical Atlantic with the ERA-Interim and observational infrared brightness temperature data from a 19-yr dataset (1990–2008 from July to September). The second question is analyzed by comparing the relative proportion of the train of the AEW troughs transformed into tropical depressions between the West African coast and 40°W. This paper is organized as follows: data used and the automatic tracking methods are presented in section 2. Section 3 gives some comparisons in the composite properties between the families of tracked systems. The relationship between tropical cyclogenesis and AEW trains is investigated in section 4. The main results of the study are discussed in section 5 and the conclusion and perspectives are presented in section 6.

## 2. Data and tracking methodology

### a. Data

The latest global atmospheric reanalysis of the ERA-Interim is used to track the systems and to build the composites over 19 summer seasons (between July and September from 1990 to 2008). Data are available on a 0.75° horizontal grid every 6 h (0000, 0600, 1200, and 1800 UTC). These data are available on 23 levels from 1000 to 200 hPa. Information about model description, data assimilation method, and input datasets used to produce ERA-Interim are documented in Dee et al. (2011).

The Cloud Archive User Service (CLAUS) is a project supported by the European Union funded to produce a long series of global infrared brightness temperature (BT) data and to validate the general circulation models. The data result from a double interpolation of operational meteorological satellites (Meteosat, GMS, and GOES-West and GOES-East) and polar-orbiting satellites

[NOAA-7, NOAA-9, NOAA-11, NOAA-8, etc., see Hodges et al. (2000) for the used interpolation methods]. They are provided on a regular horizontal grid of 0.5° in longitude and latitude with 3 h of temporal resolution and currently cover the period 1 July 1983 to 30 June 2009. The data are widely used in West Africa and in the eastern Atlantic regions (Hodges and Thorncroft 1997; Lavaysse et al. 2010; Hopsch et al. 2010; Dieng et al. 2014). These data are provided by the Institut Simon Laplace (IPSL; <http://climserv.ipsl.polytechnique.fr>).

Information about named TCs is provided by The NOAA/National Hurricane Center (NHC) best track archives that summarize the dates of occurrence and tracks of North Atlantic TCs. Note that only tropical storm genesis, which occurs in the vicinity of the West African coast (east of 40°W), is considered.

### b. Tracking methodology

#### 1) DETECTION REGION AND STUDY PERIOD

Figure 1 shows the map of the western African continent and the Atlantic Ocean. The systems are tracked from the West African coast to the central Atlantic Ocean (large dotted rectangle in Fig. 1). However, only those systems coming from West African coasts between 13.5° and 18°W are studied. Also, tracking has been limited to 20°N to avoid disturbances originating from the mid-latitudes regions, which can penetrate into the tropics during the summer period (see Diedhiou et al. 1999). Approximately 2000 km from the coast (around 36°W), a second zone of the same longitudinal width as the coastal one is chosen to find the systems that may precede these coastal systems. Indeed, this distance was found by Vizy and Cook (2009) as the mean distance separating pre-Tropical Storm Debby and Tropical Storm Ernesto in the case of Tropical Storm Debby genesis, and was confirmed by Dieng et al. (2014) with a composite analysis.

The July–September period is chosen to focus on tropical depression peak formation in the tropical Atlantic.

#### 2) TRACKING METHODOLOGY

Fluctuations associated with the AEWs passage can be detected locally in a large number of measured in situ variables (e.g., the components of the 700- or 850-hPa meridional wind speed, surface pressure, relative vorticity, geopotential, precipitable water, etc.). A commonly used method for identifying AEWs trough is to find where the meridional wind at the level of the AEJ is equal to zero. That location usually determined at 700 and at 850 hPa for the northern and southern AEW tracks, respectively, defines the wave trough, where the wind shifts from northerlies to southerlies (Diedhiou et al. 1999). The horizontal distributions of streamlines of unfiltered

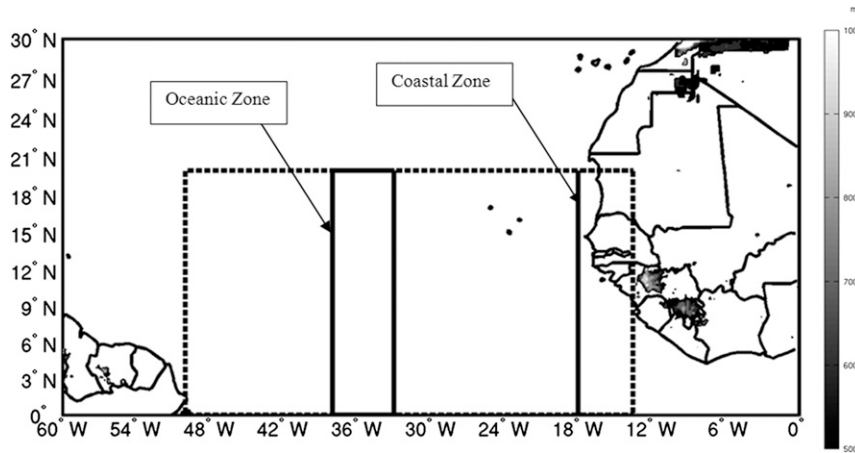


FIG. 1. Map of West Africa and the tropical Atlantic basin including the areas where systems are selected and tracked. The relief over 500 m is shaded. The large, dotted rectangle indicates the region where the systems are tracked. The two small rectangles represent the detection area of systems (see text in section 2 for details).

wind are also used to detect the AEW trough signature (Reed et al. 1977, 1988; Fink and Reiner 2003; Fink et al. 2006). Since AEW troughs are also marked by cyclonic circulation at 700 hPa, the relative vorticity at this level is often used to detect and track AEW signatures (Thorncroft and Hodges 2001; Berry and Thorncroft 2005; Hopsch et al. 2007; Arnault and Roux 2011). It should be noted, however, that AEWs are intrinsically dynamical disturbances that are strongly affected by

interactions with convection. Therefore, satellite Tb is also used to detect the AEWs signatures.

The selection and tracking methodology were based on criteria applied to ERA-Interim relative vorticity and CLAUS brightness temperature fields. Various tests were performed to get the most consistent tracking strategy. The spatiotemporal tracking procedure was done using the Matlab function `bwlabeln` (Haralick and Shapiro 1992). Based on threshold criteria, the processing

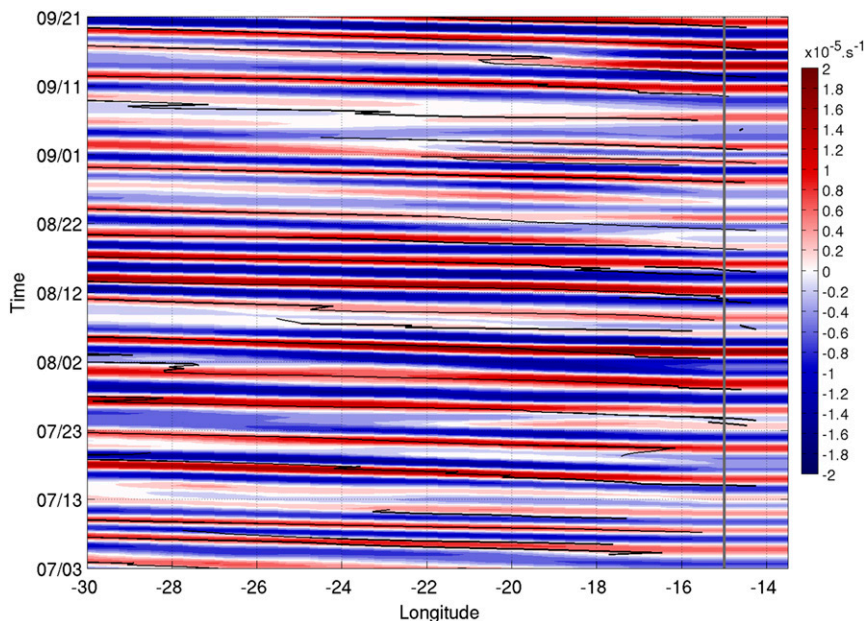


FIG. 2. Time-longitude diagram of 700-hPa 2–6-day bandpass-filtered relative vorticity ( $\times 10^{-5}$ ) averaged between 5° and 15°N on which are overlaid the tracks (black lines) of systems for the period of July–September 2000.

starts at the first grid point of the first field date of each season. Then it spreads throughout the rest of the data field based on the connectivity of the grid, then to the successive fields as well. Connectivity defines distinct “objects,” in space and time.

The tracking was applied to

- 1) 700-hPa relative vorticity anomalies (after removing the seasonal trend);
- 2) 700-hPa vorticity anomalies (after removing the seasonal trend), but the presence of Tb and water vapor anomalies are checked along the path of the 700-hPa tracked vortex;
- 3) 700-hPa relative vorticity, temporarily filtered between 2 and 6 days and checking presence of Tb and water vapor anomalies as done in the previous step; and
- 4) Tb anomalies, then checking the presence of a vorticity maximum and water vapor anomalies along the track of Tb anomalies.

The threshold choice is a delicate topic because it depends on several factors such as the type of data used (filtering the vorticity field or taking anomalies etc.) A threshold too low provides many indiscernible systems whereas a high threshold gives very a small amount of systems leading to underestimating the total number. The threshold choice must therefore be chosen in order to get the maximum of systems, but keeping their overall consistency. Some criteria then can be added to select the systems of interests according to the objectives. For example, many authors use the lifetime and the traveled distance by the disturbances to eliminate those that are not related to AEWs after making a first selection with the relative vorticity (Thorncroft and Hodges 2001; Hopsch et al. 2007; Guy et al. 2011; Berry and Thorncroft 2012). In the present study, thresholds are mainly based on the results of the composite of strengthening MCS, embedded in AEW trough, observed near the West African coast by Dieng et al. (2014). These composites were built from intraseasonal anomalies in the ERA-Interim by removing at each gridded point of data the corresponding 30-day moving average.

The difference between the first and the second method is the presence of Tb and precipitable water vapor anomalies inside the surface vortex along its lifetime. The comparison of lifetime between the two populations shows that the presence of these anomalies can significantly filter short lifetime systems. However, the intraseasonal anomalies do not allow filtering of the large structures in the 700-hPa vorticity fields that are used for systems tracking. Therefore the tracks in both methodologies were not smoothed. According to Janiga and Thorncroft (2013), temporal bandpass filtering eliminates large-scale fluctuations that are not related to synoptic-scale disturbances

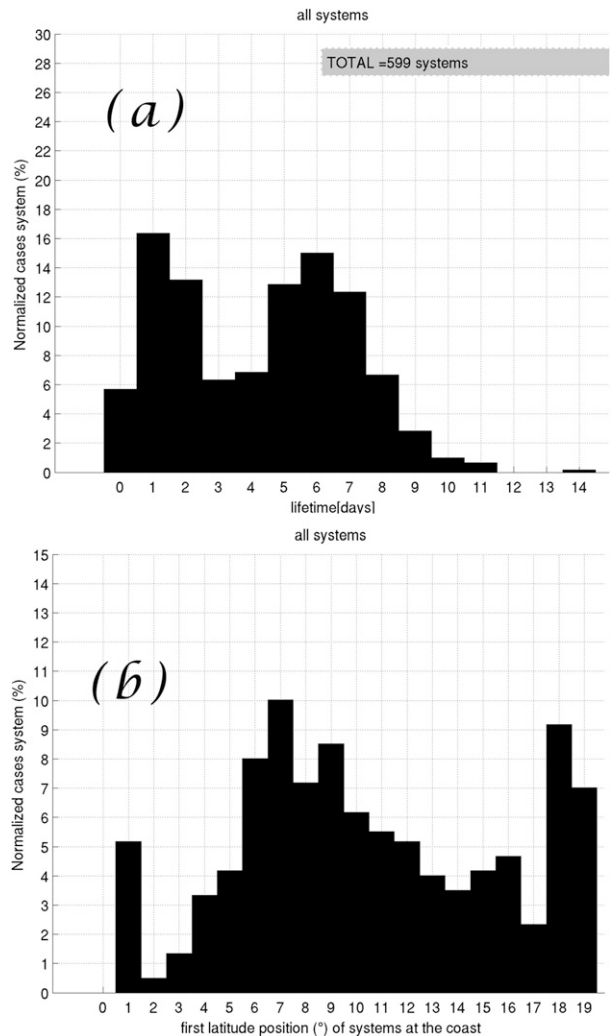


FIG. 3. Normalized histogram of (a) lifetime and (b) latitude position at the coast for all tracked systems during the July–September period from 1990 to 2008.

and then improves the quality of trajectories. The first and the second approach were therefore eliminated. The fourth one was also eliminated, because it led to shorter trajectories than the first and third ones. The reason is that Tb anomalies are not as smooth in space and continuous in time (the time spacing is 6 h in reanalyses). The function was thus applied on the 700-hPa bandpass-filtered relative vorticity fields of each season to obtain trajectories of the AEW trough to study all AEWs and/or MCSs that are likely to strengthen between the West African coast and the tropical Atlantic basin for July–September periods from 1990 to 2008 with the following criteria:

- First, a  $1.0 \times 10^{-5} \text{ s}^{-1}$  threshold in 2–6-day filtered relative vorticity at 700 hPa is used to temporally and spatially track (at every 6 h with grid spacing of  $0.75^\circ$ )

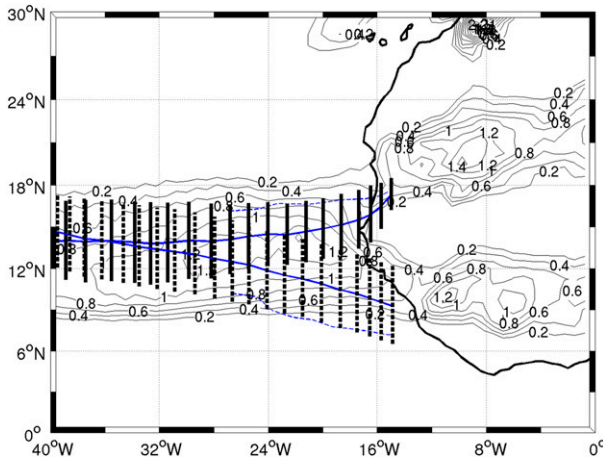


FIG. 4. Mean July–September horizontal structure of positive relative vorticity at 850 hPa, on which are tracked the mean trajectories of four identified families of system: the dashed lines represent the SLS and solid lines are for LLS. The black vertical lines represent the latitudinal standard deviation of north-LLS and south-LLS tracks.

any AEWs propagating from the West African coast to the central tropical Atlantic.

- To ensure that selected AEWs troughs are associated with convective activity, a threshold of  $-3\text{ K}$  in brightness temperature anomaly and of  $0.5\text{ kg m}^{-2}$  in precipitable water anomaly are applied along the vortex of every tracked system to eliminate those that are not associated with convective activity or evolving in a dry environment, respectively. This condition eliminates numerous systems with short lifetimes. All small systems, which extend on less than six grid meshes in ERA-Interim fields, were not considered for this study. In addition, according to several previous studies, such systems are not expected to develop.

The center of the system (convection imbedded in a positive vorticity area) is determined as the geographical center of the negative  $T_b$  anomaly inside the vorticity maximum area. An example of seasonal tracking is shown in Fig. 2: the longitude–time plot is made in average on the  $5^\circ\text{--}15^\circ\text{N}$  latitude band. The relative vorticity is shown, with the center of the convection area embedded in it. Note the presence of a few jumps in some trajectories due to the interaction between the AEW trough and convection

(Berry and Thorncroft 2005; Berry et al. 2007; Berry and Thorncroft 2012). These shifts could be due to the effect of averaging the relative vorticity field on a wide latitude band ( $5^\circ\text{--}15^\circ\text{N}$ ), which could mix northern and southern systems in the same region. The large majority of these systems are well located, along their trajectory, in the trough of the AEW with which they are associated. Therefore, these trajectories can be used for statistical analyses of the AEW trough and embedded convection.

Figure 3a shows the lifetime histogram of all systems over the 19 seasons. Based on our methodology, 599 troughs with embedded MCS have crossed the West African coast between July and September from 1990 to 2008. This represents on average 32 systems per season, which is consistent with the mean periodicity of AEWs. For simplicity, we define a short life span system (SLS), which has a lifetime shorter than 4 days, and a long life span system (LLS), which has a lifetime longer than 4 days. The SLS represent 43% while LLS represent 57% of the total population.

Figure 3b shows the distribution of latitudinal location of the systems at the coast (around  $15^\circ\text{W}$ ). We note that these positions mainly occur at two zones: 1) around  $9^\circ\text{N}$  and 2) at around  $18^\circ\text{N}$ . These zones correspond to the latitudinal tracks of AEWs moving on either sides of the AEJ (Carlson 1969; Reed et al. 1988; Thorncroft and Blackburn 1999; Thorncroft and Hodges 2001; Diedhiou et al. 2001; Chen 2006; Hall et al. 2006, and others). Considering these differences and in order to better isolate the properties of each group, the systems evolving in the north zone and those evolving in the south are separated into two groups as follow: the south systems are those originating between the equator and  $15^\circ\text{N}$  and the north systems are those from  $15^\circ$  to  $20^\circ\text{N}$ . Finally, this gives us four main cases of systems:

- Short life span system originating from the north zone (north-SLS);
- Long life span system originating from the north zone (north-LLS);
- Short life span system originating from the south zone (south-SLS);
- Long life span system originating from the north zone (south-SLL).

TABLE 1. Parameters and thresholds used for the automatic tracking.

Thresholds	Parameters		
	2–6-day filtered relative vorticity ( $10^{-5}\text{ s}^{-1}$ )	Brightness temperature anomaly (K)	Precipitable water anomaly ( $\text{kg m}^{-2}$ )
At the coastal zone	1	$-3$	0.5
At the oceanic zone (only for DUO cases)	0.3	$-1$	0.2

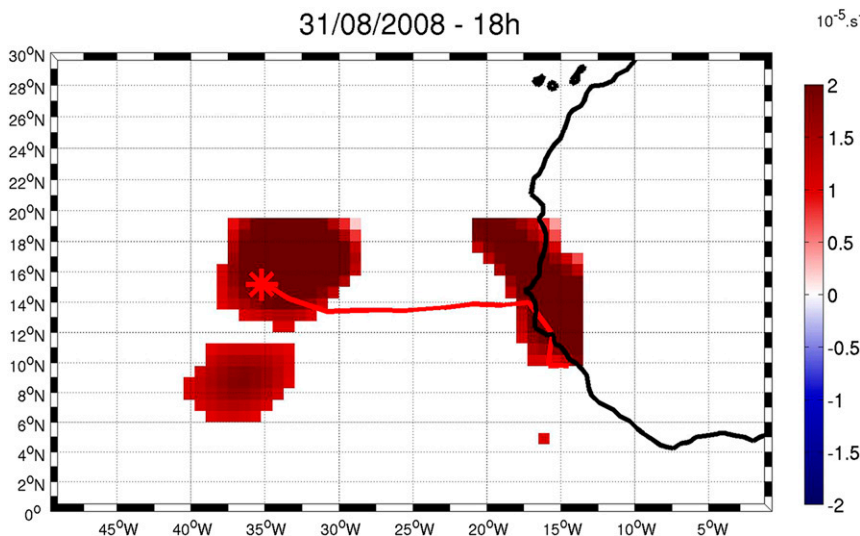


FIG. 5. Example of instantaneous detection of two consecutive AEW troughs at 1800 UTC 31 Aug 2008. The 700-hPa 2–6-day bandpass-filtered relative vorticity ( $\times 10^{-5}$ ) associated with troughs are shaded. The red star is the center of the system determined as the geographical center of the Tb anomaly inside the vorticity maximum area.

Figure 4 shows the mean July–September horizontal structure of positive relative vorticity at 850 hPa, on which are plotted the mean trajectories of the four identified families of the system: the dashed lines represent the SLS and solid lines are for LLS. We can

observe that these trajectories are located in the positive 850-hPa relative vorticity field, with signatures of the two AEWs track traveling on either side of the AEJ [the mean position of the AEJ is 15°N according to Kiladis et al. (2006), see their Fig. 2].

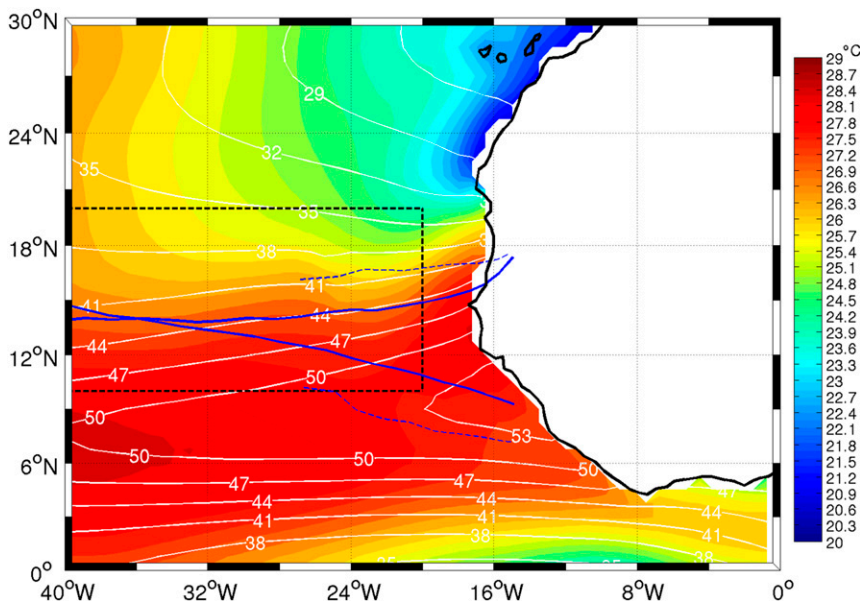


FIG. 6. Horizontal structure of mean July–September from 1990 to 2008 of SST (local, ranging between 20° and 29°C) and of total column water vapor (white contours). Overlaid over these fields are the mean trajectory of LLS (north and south blue solid lines) and the mean trajectory of SLS (north and south, blue dashed lines).

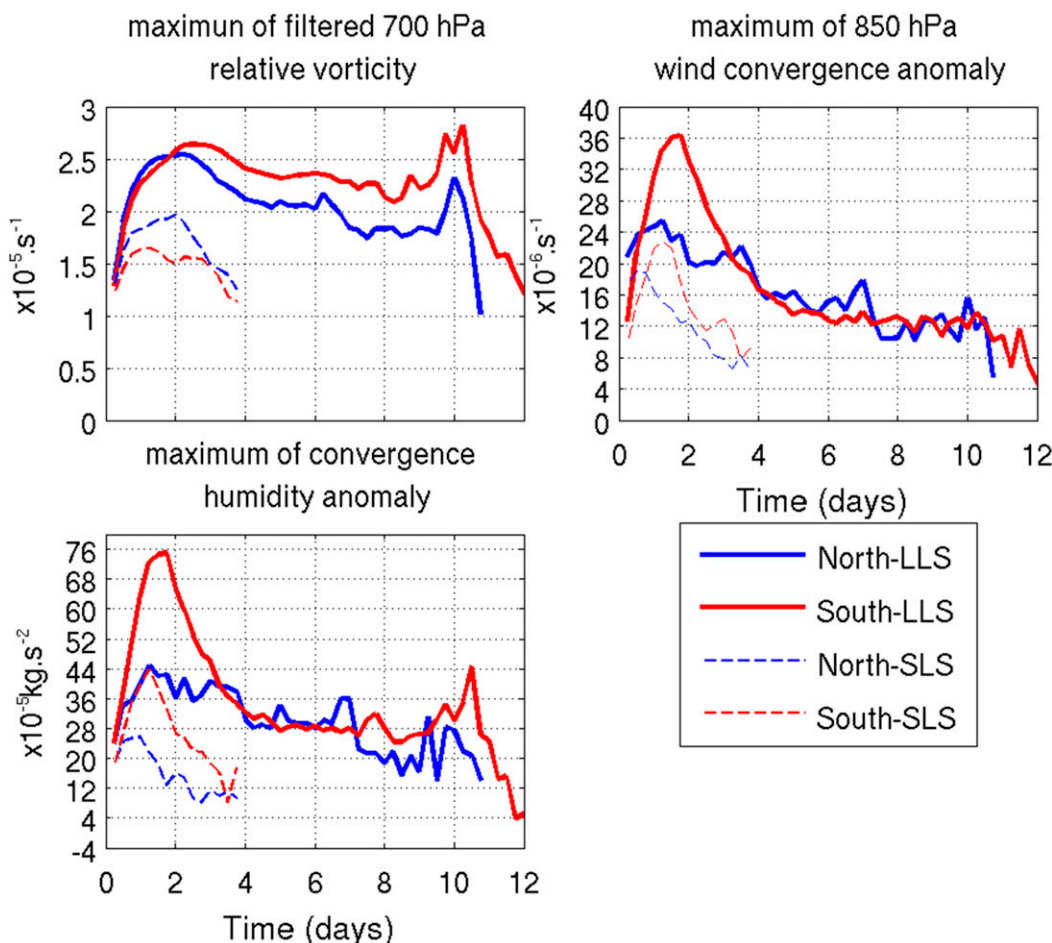


FIG. 7. Maximum anomalies in the 700-hPa vortex area of systems. The blue lines are for systems coming from the south zone and red lines are for systems coming from the north zone. Solid and dashed lines represent LLS and SLS, respectively. Presented in anomalies: (top left) 700-hPa relative vorticity, (top right) 850-hPa wind convergence, and (bottom left) surface–850-hPa convergence humidity flux.

### 3) IDENTIFICATION OF DUO AND SOLO SYSTEMS

Following the recent results of Peng et al. (2006), Vizi and Cook (2009), and Dieng et al. (2014), we analyze the relationship between the system's lifetime and the successive AEW trough occurrence by comparing the mean properties of systems that are associated with a downstream trough located around 2000 km westward, and those that are not associated with such a close downstream trough. For this goal, all of the 599 detected systems are separated into two classes: the first class gathers systems that are preceded by a previous system at approximately 2000 km downstream from the coast (see section 2b), at the same time as they cross the coast. However, because of the objective detection, the system associated with weak anomalies cannot be taken into account as DUO with this criterion. In order not to overlook any DUO cases, a second criterion has been

established. This consists of taking into account any system as DUO if it is associated with a positive relative vorticity anomaly and precipitable water at 2000 km, at the moment it crosses the coast (see Table 1 for the used thresholds). Figure 5 is an example of the simultaneous detection of two consecutive disturbances at 1800 UTC 31 August 2008. In the following, the systems satisfying this condition will be noted hereafter as “DUO systems.” The second class (termed hereafter as “SOLO systems”)

TABLE 2. Repartition of AEWs trough families detected over the West African coast during the Jul–Sep period from 1990 to 2008.

	North-LLS	North-SLS	South-LLS	South-SLS
DUOS	65	20	163	97
SOLO	35	33	80	106
Total	100	53	243	203

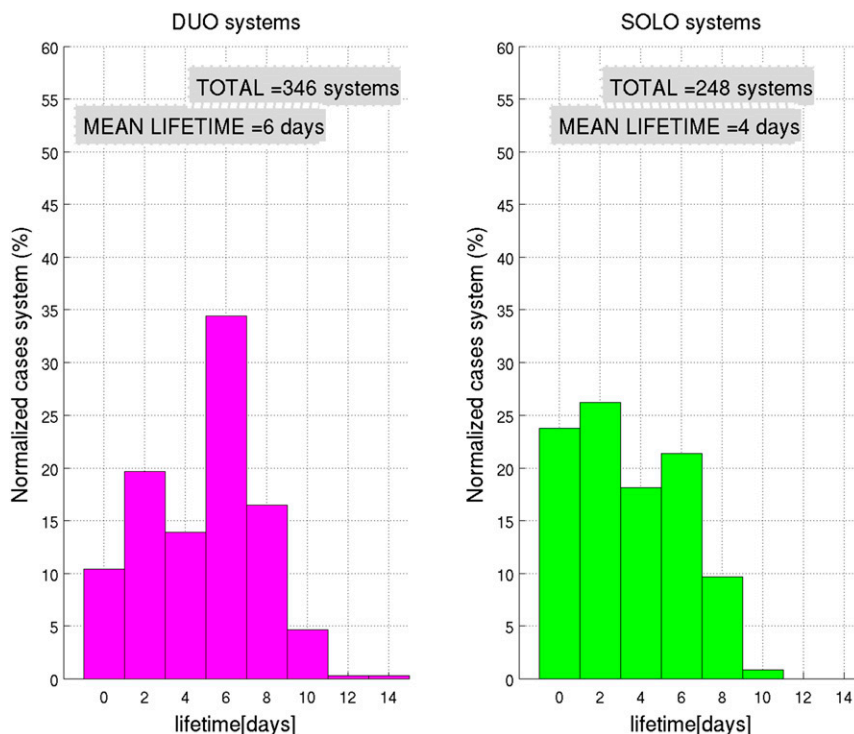


FIG. 8. Standardized histogram of lifetime: (left) for DUO systems and (right) for SOLO systems.

gathers the systems that the preceding one cannot interact with because the distance between them is too great.

### 3. Results

#### *a. Relationship between the lifetime of a system and its origin*

In this section we try to understand why SLSs (coming from the north or from the south zone) do not last long (less than 4 days) over the ocean. In addition we discuss the main difference between the systems coming from the north and those coming from the south zone.

Table 1 shows the distribution of systems with regard to their origin in latitude. The north systems represent 26% of the total population while the south systems represent 74% of the total population. These proportions suggest that the north system family is underestimated according to the results of Chen et al. (2008). The limitation at 20°N and the pressure level used in the tracking method are probably the factors responsible for the underestimation.

Figure 6 shows the mean July–September horizontal structure of sea surface temperature (SST) and of precipitable water vapor (specific humidity integrated from the surface to 100 hPa). The area of the MDR is

represented by the black dashed rectangle. We note that the north-SLS and the south-SLS evolve at the northeastern and at the southeastern part of the MDR, respectively. The northeastern part of the MDR is marked by a predominance of local low humidity (precipitable water vapor less than  $40 \text{ g kg}^{-1}$ ) and relatively cold waters (SST ranging between 25° and 26°C). Therefore, these unfavorable conditions could be responsible for the decay of the north-SLS in this zone. Although the south-SLS are evolving in better conditions (high humidity and greater SST), their mean trajectory suggests that they mainly propagate outside of the MDR, in the southern part, where the Coriolis force is less important. Thus, the absolute vorticity ( $\zeta_a = \zeta_r + f$ , where  $f$  is the Coriolis parameter and  $\zeta_r$  is the relative vorticity) associated with these systems should be weaker causing their short life span. Regarding the systems lasting more than 4 days over the ocean (solid line), the north-LLS and south-LLS remain in the MDR following a west-southwest and west-northwest direction, respectively, to merge around 36°W (approximately 2000 km from the coast). This area corresponds to the second peak in genesis density of AEW observed by Hopsch et al. (2007). This result also could confirm the results of Chen et al. (2008) who found with a manual tracking method that the AEW<sub>n,s</sub> are

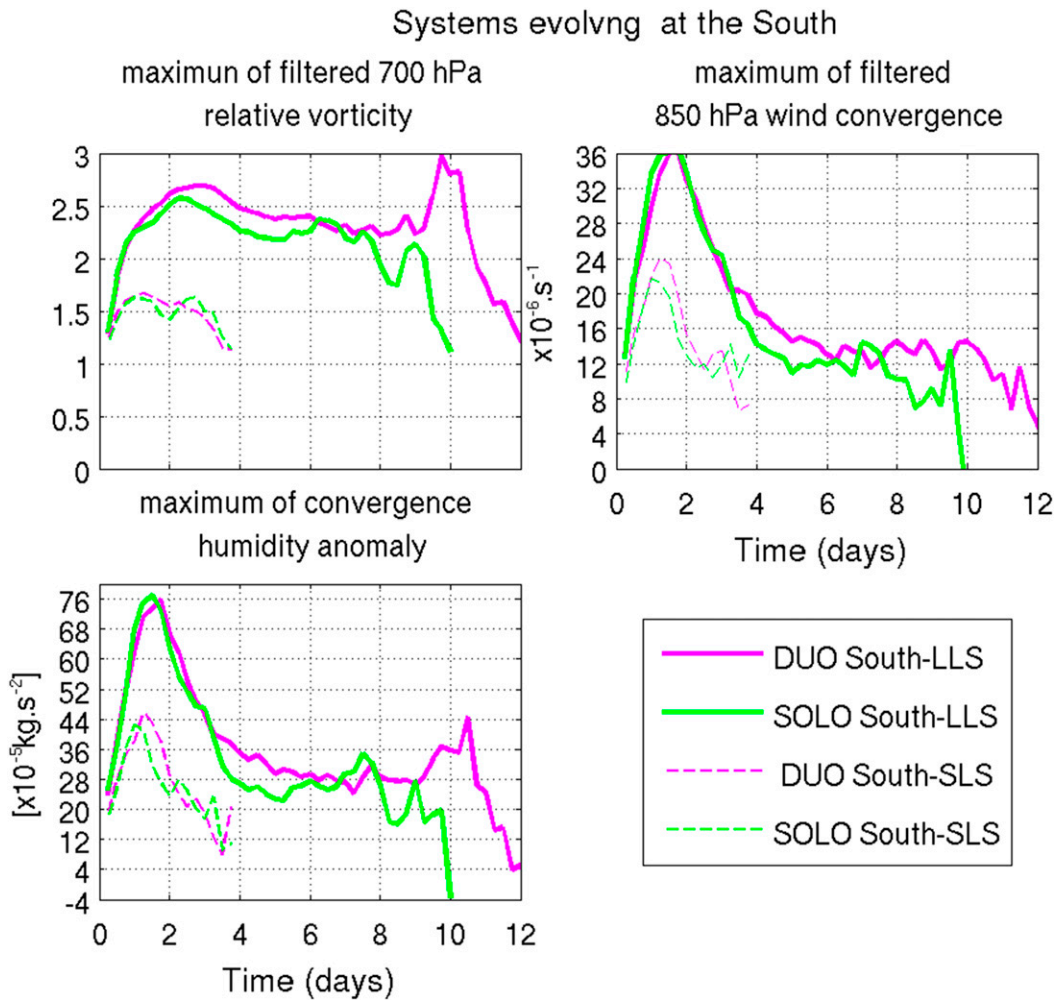


FIG. 9. Mean anomaly in the 700-hPa vortex of the system. Magenta is for DUO systems and green is for SOLO systems. Solid and dashed lines represent LLS and SLS, respectively. Presented in the anomaly: (top left) 700-hPa relative vorticity, (top right) 850-hPa wind convergence, and (bottom left) surface–850-hPa convergence humidity flux.

clustered along the ITCZ between 30°E and 50°W. However, as shown in the latitudinal standard deviation of long life system tracks shown in Fig. 4, some north systems can merge with south systems in the vicinity of West African coasts, as observed by Chen and Liu (2014).

Figure 7 shows the maximum anomaly along trajectories of four families of systems, covered in their 700-hPa vortex. During the early days of evolution, the south-LLS present more intense dynamic structures than the north-LLS suggesting that the south zone is more favorable for the system initial development (before the fourth day) than the north zone, in agreement with Hopsch et al. (2007) who showed that most tropical storms that reach the MDR come from the south zone.

#### b. Comparison between DUO and SOLO systems

In this subsection we address some responses to the first question of the introduction by comparing properties between DUO systems (system with a previous system) and SOLO systems (system without a previous one). However, because of the underestimation of north systems, the comparison results of system coming from the south zone will only be discussed hereafter.

##### 1) STATISTICAL RESULTS

Table 2 and Fig. 8 show the proportion between the system categories and the standardized histogram of lifetime for the DUO systems (left figure) and for the SOLO systems (right figure). The DUO cases represent 58% of total population and the SOLO cases represent

Horizontal structure at 700hPa

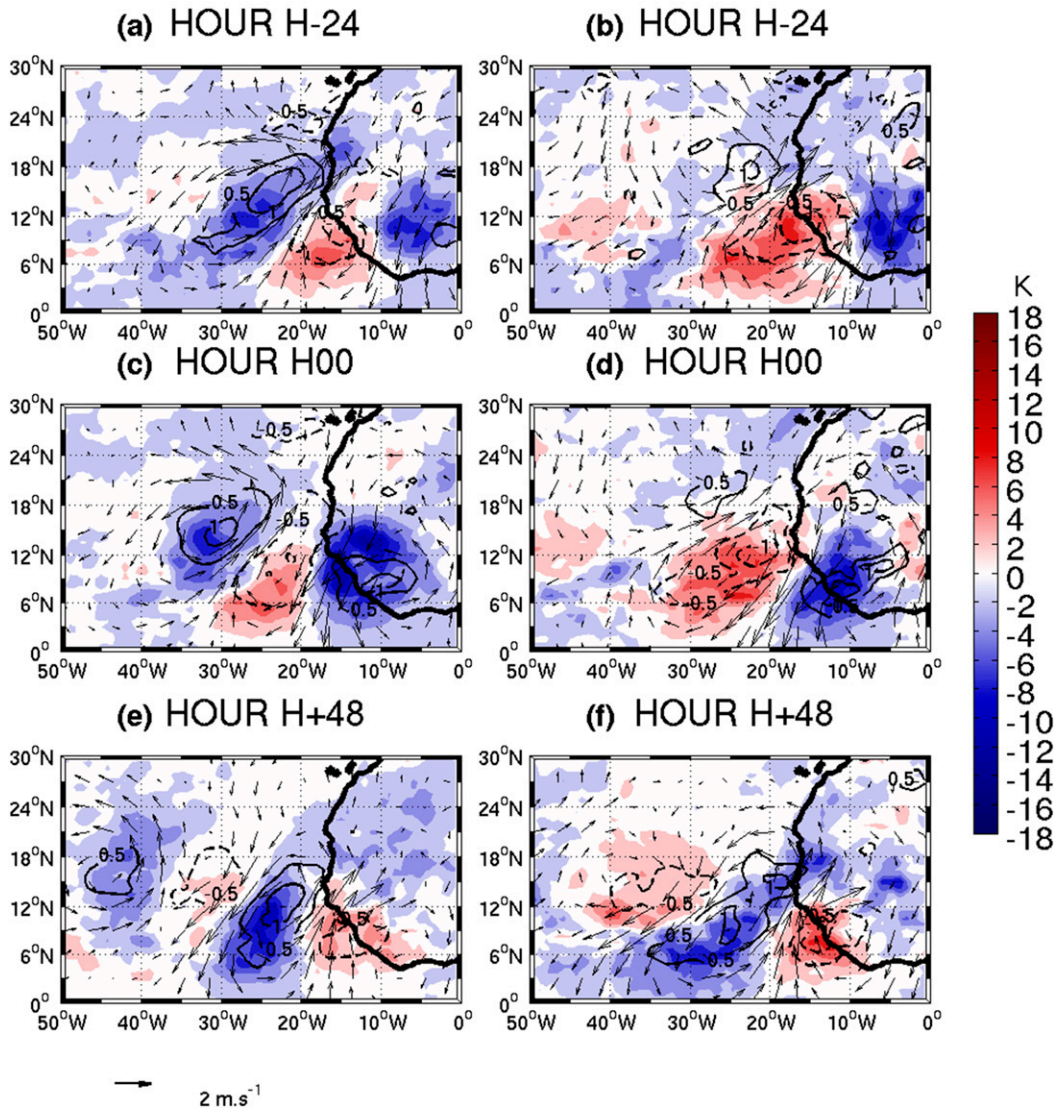


FIG. 10. Composites of brightness temperature anomaly (colors, K) at 700 hPa of wind anomaly (arrows,  $m s^{-1}$ ) and relative vertical vorticity anomaly (contours,  $\times 10^{-5} s^{-1}$ ) at (a),(b)  $H - 24$  h; (c),(d)  $H00$ ; and (e),(f)  $H + 48$  h for (left) DUO south-LLS and (right) SOLO south-LLS. The horizontal (vertical) axis (in  $^{\circ}$ ) is longitude (latitude).

42%. Note that 58% of DUO cases have a lifetime more than 4 days, while 31% of SOLO cases have a lifetime of more than 4 days. Moreover, the mean lifetime of all DUO cases is 6 days whereas it is 4 days for the SOLO cases (Fig. 8). A Student's  $t$  test confirms that this difference is statistically significant at the 90% level. These results suggest that, over the ocean, the DUO systems last generally longer than the SOLO systems.

2) MEAN PROPERTIES ALONG TRAJECTORIES

Figure 9 shows the maximum anomaly in the 700-hPa vortex area along the trajectory of south DUOS and south

SOLO cases. During their evolutions, the DUO cases exhibit slightly stronger 700-hPa relative vorticity, 850-hPa wind convergence, and surface–850-hPa humidity flux anomalies suggesting that the DUO systems have stronger dynamic structures than the SOLO systems.

3) MIDLEVEL HORIZONTAL STRUCTURE

In this section, the horizontal structures of cases systems are compared. Composite fields are built, as previously done by Dieng et al. (2014), by overimposing the fields at the time the system cross the coast. Contrary to the previous study, the latitude variation does not need

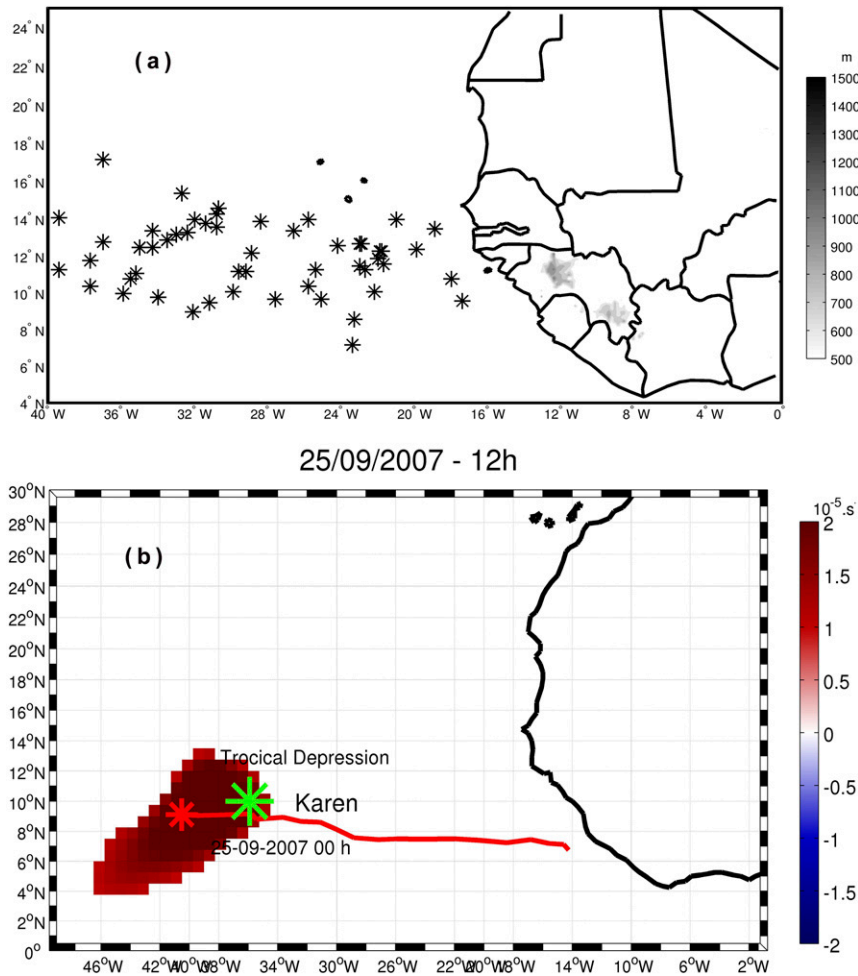


FIG. 11. (a) First positions of declared tropical depressions by the National Hurricane Center (NHC) best track during the July–September period from 1990 to 2008. (b) Mean trajectory of a system that transformed to Tropical Depression Karen at 1800 UTC 25 Aug 2007. The 700-hPa 2–6-day bandpass-filtered relative vorticity ( $\times 10^{-5}$ ) associated with the trough is shaded.

to be corrected for, since north and south systems are not mixed together.

Figure 10 shows the spatiotemporal evolution of the composite structure at 700 hPa at  $H - 24$  h (Figs. 10a,b), H00 (Figs. 10c,d), and at  $H + 48$  h (Figs. 10e,f) for DUO south-LLS (Figs. 10a,c,e) and for SOLO south-LLS (Figs. 10b,d,f). At  $H - 24$ , in the DUO cases (left panels), the previous system (first trough) is located off the West African coast near Cape Verde (near  $30^{\circ}\text{W}$ ). It is associated with convective activity (negative anomaly of brightness temperature) and a positive relative vertical vorticity anomaly (Fig. 10a). At the same time the DUO south-LLS (second trough) is still over the continent, approximately at  $10^{\circ}\text{N}$ ,  $5^{\circ}\text{W}$ . Between the two systems, an anticyclonic circulation is developed, centered at  $9^{\circ}\text{N}$ ,  $18^{\circ}\text{W}$ . This anticyclonic circulation associated with drier air (not shown) corresponds to the

ridge sector of the AEW. From  $H - 24$  to  $H + 24$ , as the AEW shifts westward and crossing the West African coast, the two troughs strengthen then weaken the ridge sector between them. Note that during this period the convection signal (negative brightness temperature anomaly) is mainly developing in the trough sector for the DUO south-LLS and between the trough and the south sector for the first system, consistent with previous studies (Reed et al. 1988; Diedhiou et al. 1999, 2001; Fink and Reiner 2003; Hall et al. 2006; Poan et al. 2013, 2015). Anomaly patterns present a clear northeast–southwest-oriented tilt suggesting that they are maintained by barotropic conversion from the AEJ (e.g., Hall et al. 2006; Leroux et al. 2010).

The composite structure of the SOLO south-LLS follows the same evolution as the DUO cases but is not associated with the preceding AEW trough by

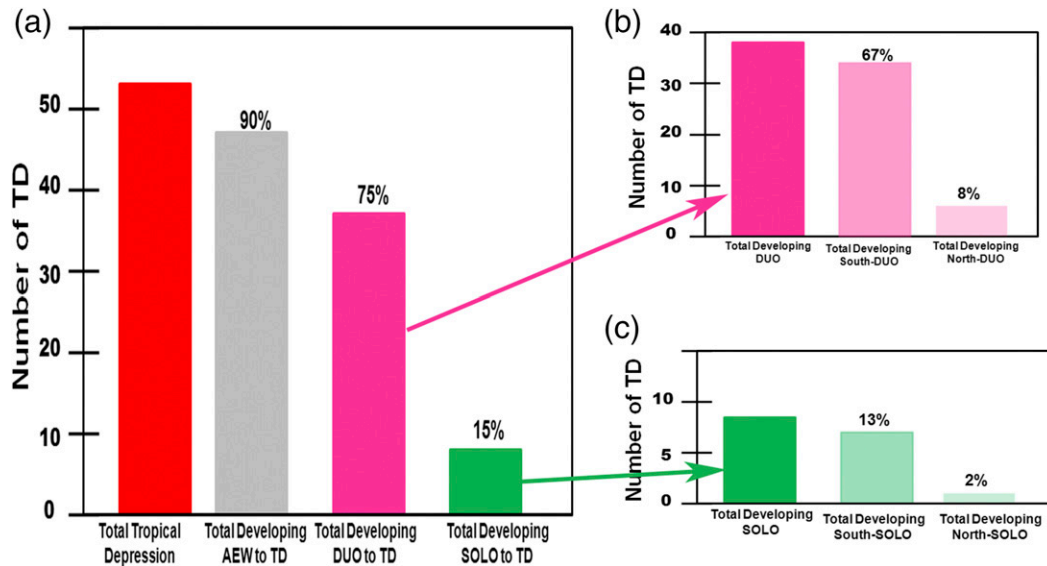


FIG. 12. (a) Occurrence of total tropical depressions (TD) (red), of total tracked system transformed to TDs (gray), of DUO systems transformed to TDs (magenta), and of SOLO systems transformed to TDs (green). (b) Proportion of south-DUO and of north-DUO systems transformed to TDs. (c) As in (b), but for SOLO systems.

definition. In this case, the relative vorticity, wind, and brightness temperature anomalies are lower, except for the ridge axis (the anticyclonic circulation) where the dissipation is less obvious (Figs. 10d–f). In addition, the SOLO ridge axis is wider than in the DUO case, and associated with a positive Tb anomaly, indicating a clear or weakly cloudy atmosphere. A small cyclonic circulation is indeed observable from  $H - 24$  to H00 downstream of this ridge, but is rapidly weakening as the ridge strengthens suggesting that its evolution is affected by the ridge amplification. Arnault and Roux (2010) show that this intense downstream ridge could contribute to the cyclonic vorticity maintenance of the subsequent AEW trough in the SOLO case.

### c. Relationship between successive wave train and downstream tropical cyclogenesis

Dieng et al. (2014) show that, the presence of a previous AEW trough west of the coast should increase the likelihood of tropical depression (TD) genesis in the vicinity of the West African coast. Figure 11a shows the spatial distribution of 52 TD genesis locations, occurring in the July–September period from 1990 to 2008. The link between these TD genesis locations and the automatically tracked systems (with the above criteria) is investigated in this section by seeking the spatiotemporal coincidence between them with a spatial range of  $2^\circ$  (in latitude–longitude) and a temporal range of 1 day. Figure 11b shows an example of an automatic detection of a tracked system transformed to the TD number 9 of the year 2007 on 14 August. This TD was later named later Tropical

Storm Karen (see <http://www.nhc.noaa.gov/archive/2007/al12/al122007.discus.009.shtml> for details).

### 1) STATISTICAL RESULTS

Figure 12 shows the statistics of tracked systems identified as TDs. We can observe that 90% of TDs formed in the vicinity of the West African coast come from AEW/MCS tracked systems (Fig. 12a), preferably from the DUO cases (representing 75% of the total systems transformed to TDs). Note that only nine TD geneses are related to SOLO systems. These results suggest that the presence of preceding systems increase the likelihood of cyclogenesis for systems crossing the West African coast, confirming the results of Dieng et al. (2014) who observed that most MCSs that strengthened in the vicinity of the West African coast are associated with intense AEWs trough to the west. Moreover, regarding Fig. 12b, we also observe that the southern cases are more strongly related to TD genesis than the northern cases, consistent with Hopsch et al. (2007).

### 2) COMPARISON BETWEEN DEVELOPING AND NONDEVELOPING SYSTEMS

Given that the DUOs evolving in the south zone are more involved in tropical depression genesis, the comparison between the developing and the nondeveloping was only made on those cases. Figure 13 shows the composite structure at 700 hPa at  $H - 24$  (Figs. 13a,b), at H00 (Figs. 13c,d), and at  $H + 48$  (Figs. 13e,f) for DUO south-LLS transformed to tropical depressions (Figs. 13a,c,e) and for the DUO south-LLS that did not

## Horizontal structure at 700hPa

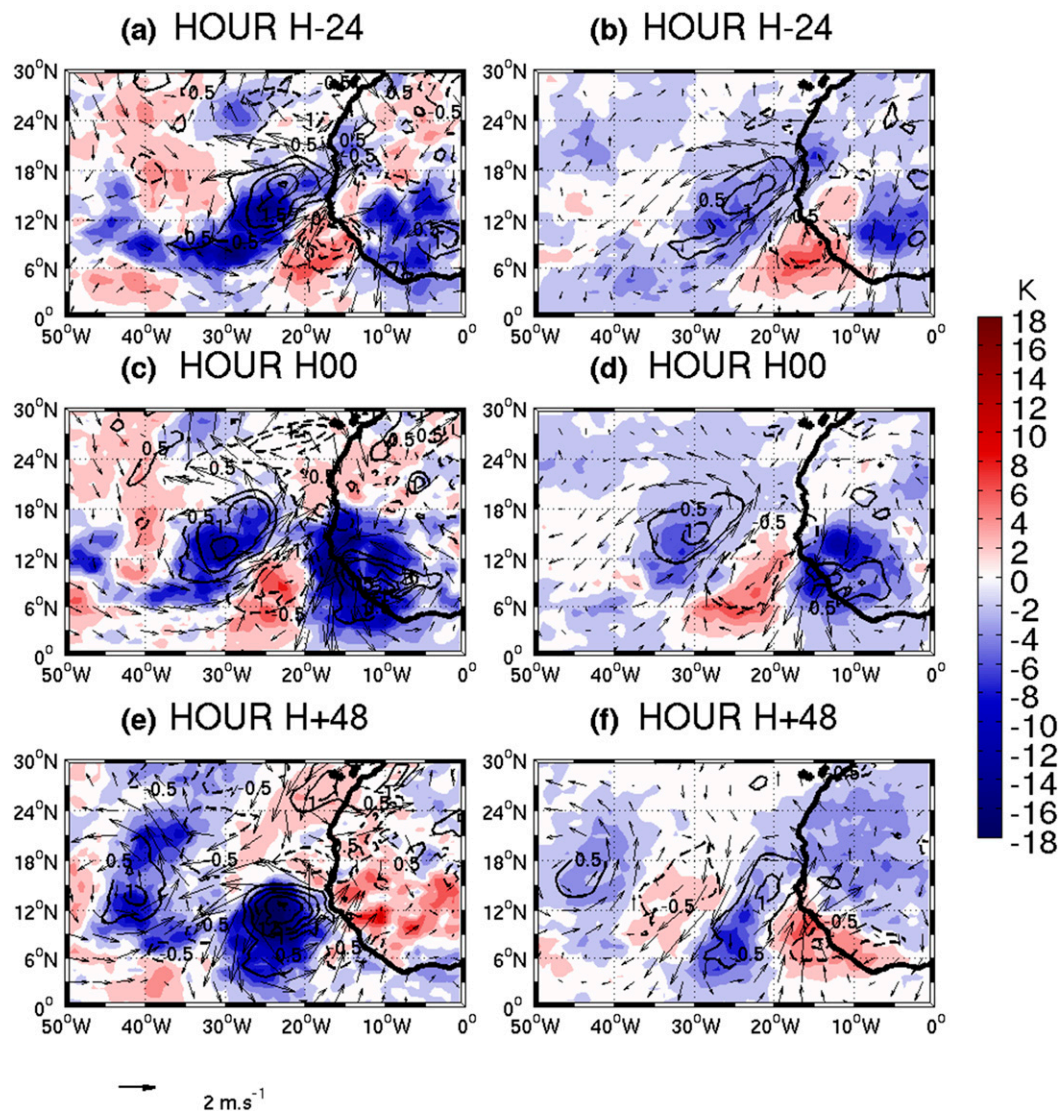


FIG. 13. Composites of brightness temperature anomaly (colors, K) at 700 hPa of wind anomaly (arrows,  $\text{m s}^{-1}$ ) and of relative vertical vorticity anomaly (contours,  $\times 10^{-3} \text{ s}^{-1}$ ) at (a),(b)  $H - 24 \text{ h}$ ; (c),(d)  $H00$ ; and (e),(f)  $H + 48 \text{ h}$  for (left) the DUO south-LLS developing to tropical depressions and (right) the DUO south-LLS nondeveloping to tropical depressions. The horizontal (vertical) axis (in  $^\circ$ ) is longitude (latitude).

(Figs. 13b,d,f). The developing systems (left) have a similar evolution as the DUO south-LLS previously analyzed (Figs. 10a–c), but here the first trough is stronger and the consecutive AEW trough evolve on the same latitude band (between  $6^\circ$  and  $17^\circ\text{N}$ ). Because of the intensification of the two AEW troughs, the ridge disappears at  $H + 48$ . At 925 hPa, the southwesterly winds anomalies of the first trough reach the northeasterly wind anomaly ahead of the second trough. Thus, the low-level wind convergence anomaly is increased from  $H00$  to  $H + 48$  (Figs. 14a and 14c). In the nondeveloping case, a ridge

remains present between the two systems, which could inhibit the low-level feeding of the main system by the previous one.

#### 4. Discussion

As shown by Vizy and Cook (2009) and Dieng et al. (2014), this study, based on 19 summer's seasons, confirms that the presence of a previous system significantly contributes to the maintenance of the systems over the ocean through moisture supply and low-level wind

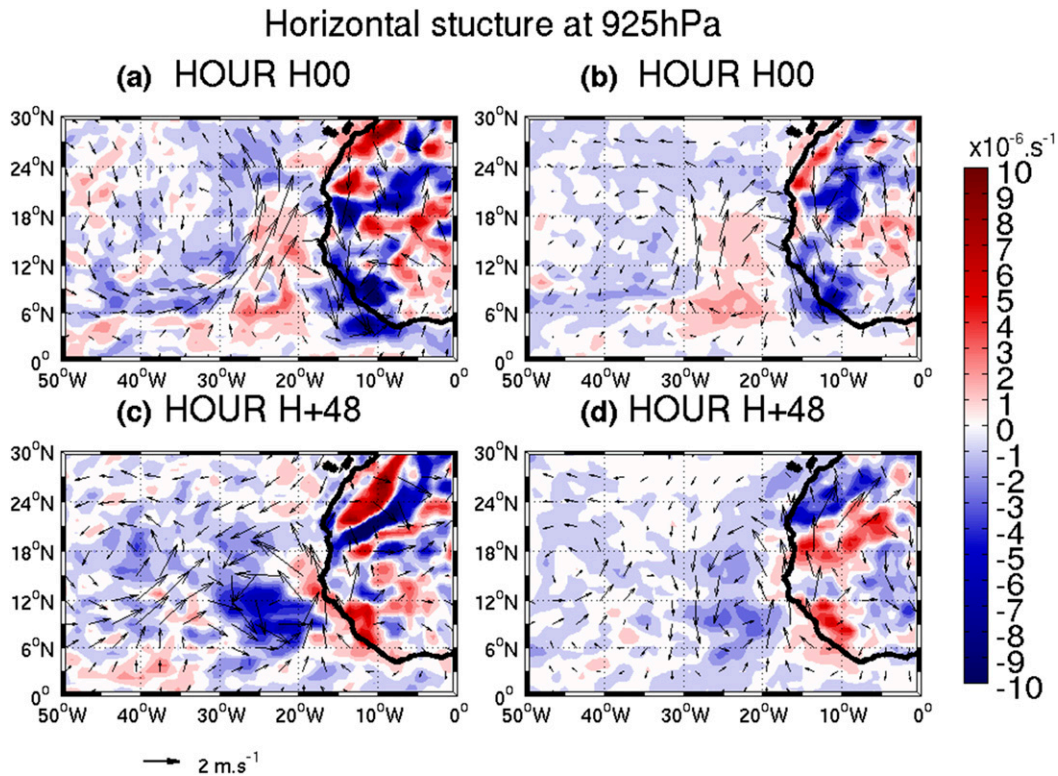


FIG. 14. Composites at 925-hPa wind divergence (colors,  $10^{-6} \text{ s}^{-1}$ ) and horizontal wind anomalies (arrows,  $\text{m s}^{-1}$ ), at (a),(b) H00 and (c),(d)  $H + 48 \text{ h}$  for the (left) DUO south-LLS developing to tropical depressions and (right) DUO south-LLS nondeveloping to tropical depressions. The horizontal (vertical) axis (in  $^{\circ}$ ) is longitude (latitude).

convergence production by the previous system. This moisture supply is accompanied by a weakening of the anticyclonic circulation between the two troughs (Fig. 10). Consequently, the reservoir of dry air associated to the Saharan air layer (SAL) is considerably weakened (not shown).

We showed that most of the tropical depressions forming in the vicinity of the West African coast are associated with previous systems. This result suggests that the presence of a previous system is an important factor for tropical cyclone genesis in the vicinity of the West African coast.

As shown in Figs. 7 and 9, all anomalies generally decrease after 2 days. This is due to the fact that only 8% (52 of 599 cases) of tracked systems are developing cases in the ensemble, so that in average the tracked systems decay after 2 days. This is why the ensemble average generally decreases after 2 days.

By looking at the latitudinal standard deviation of tracks in Fig. 4, we can observe that northern and southern trajectories can merge near the coast. This phenomenon was observed in some genesis cases (figures not shown).

The presence of a strong anticyclonic circulation (ridge of AEW) ahead of SOLO cases could in this case

contribute to its midlevel cyclonic vorticity production. By analyzing vorticity budgets in a developing and a non-developing AEW trough during their passages over the West African coast, Arnault and Roux (2010) found that the horizontal advection induced by the close ridge of AEW was larger in the developing case in which the outward transport of vertical vorticity was considerably important. An analysis of absolute vorticity budgets could clarify the role of the strong ridge associated with SOLO cases.

**5. Conclusions**

This study aimed to investigate the relationship between African easterly waves (AEWs) and downstream tropical cyclogenesis. The ERA-Interim reanalysis fields and brightness temperature data from CLAUS are used to detect and track the AEWs trough and embedded convection from the West African coast to the central tropical Atlantic. The tracked systems are separated into eight groups by considering:

- 1) their lifetimes: Systems with lifetimes longer than 4 are called long life span systems (LLS), and those with lifetimes less than 4 days are called short life span systems (LLS);

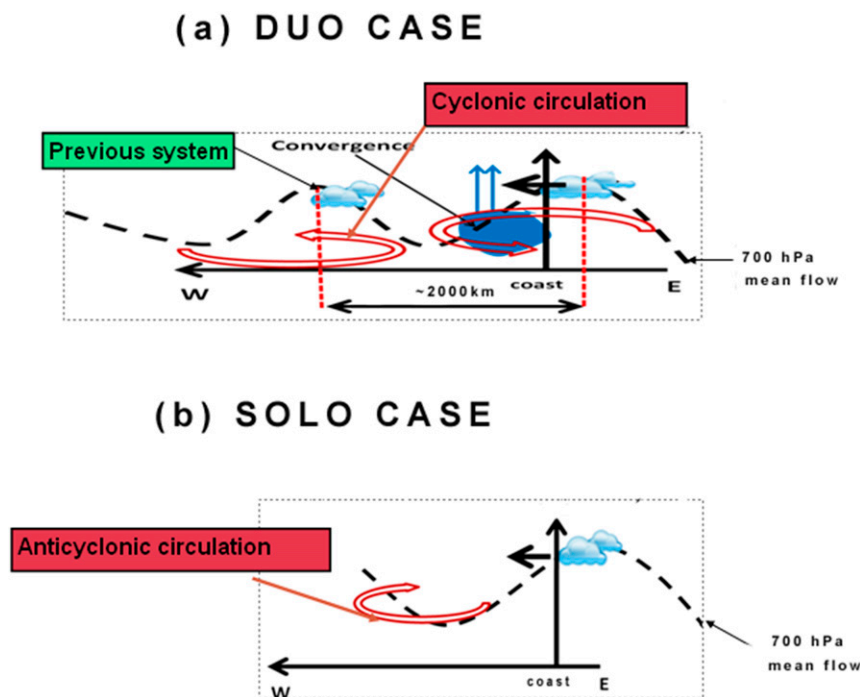


FIG. 15. Conceptual scheme of circulation of an AEW (dashed line) and embedded MCS (cloud sketch image). The red circular arrows represent the low-level circulation (around 850 hPa) (a) for the DUO and (b) for the SOLO case.

- 2) their relative position with regard to 15°N when they cross the coast;
- 3) their relationship to trains of African easterly waves: systems that are associated with close intense AEW troughs downstream are termed DUO systems and those that are not associated are called SOLO systems; and
- 4) their relationship with tropical depression genesis occurring near the West African coast.

The intercomparison between these families of systems was performed by analyzing the following:

- Their lifetimes;
  - Their dynamic structures embedded in their 700-hPa vortex core, along their trajectories;
  - Their composite structures.
- 1) Comparison between the DUO and the SOLO systems shows that the DUO systems have a longer lifetime than the SOLO systems. The analysis of relative vorticity, 850-hPa wind convergence embedded in the 700-hPa vortex along trajectories show that the DUO cases have stronger dynamical structures anomalies.
  - 2) It is shown that the systems crossing the coast farther north (beyond 18°N), cannot evolve for long over the ocean due to the predominance of cold water and

- drier air occurring in this region. Also, systems leaving the coast near the equator do not last long as they do not have a sufficient Coriolis force to be self-sustained. Comparison between systems coming from the north and those coming from the south with regard to the mean position of the AEJ, showed that the south systems present stronger dynamical structures.
- 3) Moreover, it is shown that the DUO cases present greater surface–850-hPa convergence flux anomaly than the SOLO cases. These results suggest in this case that the presence of a previous trough of AEW is a majority condition for the strengthened systems near the West African coast. Regarding the SOLO systems, the presence of an intense downstream ridge prevented any moisture supply from the west. However, composite structures associated with SOLO systems, living long over the ocean (SOLO LLS), show that they have a more pronounced downstream ridge. This ridge could contribute to their relative vorticity production.
  - 4) The analysis of the relationship between tropical depression genesis and tracked system family shows that 90% of tropical depressions forming between the West African coast and 45°W come from tracked systems while most of them are DUO cases (representing 75% of the total detected tropical depressions)

coming from the south zone. This suggests that tropical cyclogenesis in the vicinity of the West African coast is strongly influenced by the train of the AEW trough.

A conceptual scheme summarizing the main differences between DUO and SOLO is proposed in Fig. 15.

A quantitative budget of absolute vorticity could clarify the downstream ridge's contribution to the maintenance of SOLO systems. We have fixed the wavelength at 2000 km, which is a particular distance for waves. A sensitivity study of the wavelength would allow for a better understanding of the processes through which the previous AEW trough influences cyclogenesis.

*Acknowledgments.* We thank Gregory Jenkins and two anonymous reviewers for their comments on the manuscript. The reanalyses and CLAUS data were obtained from the Institut Pierre Simon Laplace (IPSL; <http://www.ipsl.fr/>). This work was funded by Centre National de la Recherche Scientifique (<http://www.cnrs.fr/>).

#### REFERENCES

- Arnault, J., and F. Roux, 2009: Case study of a developing African easterly wave during NAMMA: An energetic point of view. *J. Atmos. Sci.*, **66**, 2991–3020, doi:10.1175/2009JAS3009.1.
- , and —, 2010: Comparison between two case studies of developing and nondeveloping African easterly waves during NAMMA and AMMA/SOP-3: Absolute vertical vorticity budget. *Mon. Wea. Rev.*, **138**, 1420–1445, doi:10.1175/2009MWR3120.1.
- , and —, 2011: Characteristics of African easterly waves associated with tropical cyclogenesis in the Cape Verde Islands region in July–August–September of 2004–2008. *Atmos. Res.*, **100**, 61–82, doi:10.1016/j.atmosres.2010.12.028.
- Berry, G. J., and C. D. Thorncroft, 2005: Case study of an intense African easterly wave. *Mon. Wea. Rev.*, **133**, 752–766, doi:10.1175/MWR2884.1.
- , and —, 2012: African easterly wave dynamics in a mesoscale numerical model: The upscale role of convection. *J. Atmos. Sci.*, **69**, 1267–1283, doi:10.1175/JAS-D-11-099.1.
- , —, and T. Hewson, 2007: African easterly waves during 2004—Analysis using objective techniques. *Mon. Wea. Rev.*, **135**, 1251–1267, doi:10.1175/MWR3343.1.
- Burpee, R. W., 1972: The origin and structure of easterly waves in the lower troposphere of North Africa. *J. Atmos. Sci.*, **29**, 77–90, doi:10.1175/1520-0469(1972)029<0077:TOASOE>2.0.CO;2.
- Camara, M., A. Diedhiou, and A. Gaye, 2011: African easterly waves and cyclonic activity over the eastern Atlantic: Composite case studies. *Int. J. Geophys.*, **2011**, 874292, doi:10.1155/2011/874292.
- Carlson, T. B., 1969: Some remarks on African disturbances and their progress over the tropical Atlantic. *Mon. Wea. Rev.*, **97**, 716–726, doi:10.1175/1520-0493(1969)097<0716:SROADA>2.3.CO;2.
- Chen, S.-H., and Y.-C. Liu, 2014: The relation between dry vortex merger and tropical cyclone genesis over the Atlantic Ocean. *J. Geophys. Res. Atmos.*, **119**, 11 641–11 661, doi:10.1002/2014JD021749.
- Chen, T.-C., 2006: Characteristics of African easterly waves depicted by ECMWF reanalyses for 1991–2000. *Mon. Wea. Rev.*, **134**, 3539–3566, doi:10.1175/MWR3259.1.
- , S.-Y. Wang, and A. J. Clark, 2008: North Atlantic hurricanes contributed by African easterly waves north and south of the African easterly jet. *J. Climate*, **21**, 6767–6776, doi:10.1175/2008JCLI2523.1.
- Chiao, S., and G. S. Jenkins, 2010: Numerical investigations on the formation of Tropical Storm Debby during NAMMA-06. *Wea. Forecasting*, **25**, 866–884, doi:10.1175/2010WAF2222313.1.
- Dee, D. P., and Coauthors, 2011: The ERA-Interim reanalysis: Configuration and performance of the data assimilation system. *Quart. J. Roy. Meteor. Soc.*, **137**, 553–597, doi:10.1002/qj.828.
- DeMaria, M., J. Knaff, and B. Connell, 2001: A tropical cyclone genesis parameter for the tropical Atlantic. *Wea. Forecasting*, **16**, 219–233, doi:10.1175/1520-0434(2001)016<0219:ATCGPF>2.0.CO;2.
- Diaz, M., and A. Aiyyer, 2013a: Energy dispersion in African easterly waves. *J. Atmos. Sci.*, **70**, 130–145, doi:10.1175/JAS-D-12-019.1.
- , and —, 2013b: The genesis of African easterly waves by upstream development. *J. Atmos. Sci.*, **70**, 3492–3512, doi:10.1175/JAS-D-12-0342.1.
- Diedhiou, A., S. Janicot, A. Viltard, P. de Felice, and H. Laurent, 1999: Easterly wave regimes and associated convection over West Africa and tropical Atlantic: Results from the NCEP/NCAR and ECMWF reanalyses. *Climate Dyn.*, **15**, 795–822, doi:10.1007/s003820050316.
- , —, —, and —, 2001: Composite patterns of easterly disturbances over West Africa and the tropical Atlantic: A climatology from the 1979–95 NCEP/NCAR reanalyses. *Climate Dyn.*, **18**, 241–253, doi:10.1007/s003820100173.
- Dieng, A. L., L. Eymard, S. M. Sall, A. Lazar, and M. Leduc-Leballeur, 2014: Analysis of strengthening and dissipating mesoscale convective systems propagating off the West African coast. *Mon. Wea. Rev.*, **142**, 4600–4623, doi:10.1175/MWR-D-13-00388.1.
- Fink, A. H., and A. Reiner, 2003: Spatiotemporal variability of the relation between African easterly waves and West African squall lines in 1998 and 1999. *J. Geophys. Res.*, **108**, 4332, doi:10.1029/2002JD002816.
- , D. G. Vincent, and V. Ermer, 2006: Rainfall types in the West African Sudanian Zone during the summer monsoon 2002. *Mon. Wea. Rev.*, **134**, 2143–2164, doi:10.1175/MWR3182.1.
- Goldenberg, S., and L. Shapiro, 1996: Physical mechanisms for the association of El Niño and West African rainfall with Atlantic major hurricane activity. *J. Climate*, **9**, 1169–1187, doi:10.1175/1520-0442(1996)009<1169:PMFTAO>2.0.CO;2.
- , C. W. Landsea, A. M. Mestas-Nuñez, and W. M. Gray, 2001: The recent increase in Atlantic hurricane activity: Causes and implications. *Science*, **293**, 474–479, doi:10.1126/science.1060040.
- Guy, N., S. A. Rutledge, and R. Cifelli, 2011: Radar characteristics of continental, coastal, and maritime convection observed during AMMA/NAMMA. *Quart. J. Roy. Meteor. Soc.*, **137**, 1241–1256, doi:10.1002/qj.839.
- Hall, N. M., G. N. Kiladis, and C. D. Thorncroft, 2006: Three-dimensional structure and dynamics of African easterly waves. Part II: Dynamical modes. *J. Atmos. Sci.*, **63**, 2231–2245, doi:10.1175/JAS3742.1.
- Haralick, R. M., and L. G. Shapiro, 1992: *Computer and Robot Vision*. 1st ed. Addison-Wesley Longman, 630 pp.

- Hodges, K., and C. D. Thorncroft, 1997: Distribution and statistics of African mesoscale convective weather systems based on the ISCCP Meteosat imagery. *Mon. Wea. Rev.*, **125**, 2821–2837, doi:10.1175/1520-0493(1997)125<2821:DAOAM>2.0.CO;2.
- , D. Chappell, G. Robinson, and G. Yang, 2000: An improved algorithm for generating global window brightness temperatures from multiple satellite infrared imagery. *J. Atmos. Oceanic Technol.*, **17**, 1296–1312, doi:10.1175/1520-0426(2000)017<1296:AIAFGG>2.0.CO;2.
- Hopsch, S. B., C. D. Thorncroft, K. Hodges, and A. Aiyer, 2007: West African storm tracks and their relationship to Atlantic tropical cyclones. *J. Climate*, **20**, 2468–2483, doi:10.1175/JCLI4139.1.
- , —, and K. R. Tyle, 2010: Analysis of African easterly wave structures and their role in influencing tropical cyclogenesis. *Mon. Wea. Rev.*, **138**, 1399–1419, doi:10.1175/2009MWR2760.1.
- Janiga, M. A., and C. D. Thorncroft, 2013: Regional differences in the kinematic and thermodynamic structure of African easterly waves. *Quart. J. Roy. Meteor. Soc.*, **139**, 1598–1614, doi:10.1002/qj.2047.
- Kiladis, G., C. Thorncroft, and N. Hall, 2006: Three-dimensional structure and dynamics of African easterly waves. Part I: Observations. *J. Atmos. Sci.*, **63**, 2212–2230, doi:10.1175/JAS3741.1.
- Landsea, C., 1993: A climatology of intense (or major) Atlantic hurricanes. *Mon. Wea. Rev.*, **121**, 1703–1713, doi:10.1175/1520-0493(1993)121<1703:ACOIMA>2.0.CO;2.
- Lavaysse, C., C. Flamant, and S. Janicot, 2010: Regional-scale convection patterns during strong and weak phases of the Saharan heat low. *Atmos. Sci. Lett.*, **11**, 255–264, doi:10.1002/asl.284.
- Leppert, K. D., D. J. Cecil, and W. A. Petersen, 2013: Relation between tropical easterly waves, convection, and tropical cyclogenesis: A Lagrangian perspective. *Mon. Wea. Rev.*, **141**, 2649–2668, doi:10.1175/MWR-D-12-00217.1.
- Leroux, S., N. M. J. Hall, and G. N. Kiladis, 2010: A climatological study of transient–mean-flow interactions over West Africa. *Quart. J. Roy. Meteor. Soc.*, **136**, 397–410, doi:10.1002/qj.474.
- Pasch, R. J., L. A. Avila, and J.-G. Jiing, 1998: Atlantic tropical systems of 1994 and 1995: A comparison of a quiet season to a near-record-breaking one. *Mon. Wea. Rev.*, **126**, 1106–1123, doi:10.1175/1520-0493(1998)126<1106:ATSOAA>2.0.CO;2.
- Peng, M. S., B. Fu, T. F. Hogan, and T. Li, 2006: On African easterly waves that impacted two tropical cyclones in 2004. *Geophys. Res. Lett.*, **33**, L11807, doi:10.1029/2006GL026038.
- Poan, D., R. Roehrig, F. Couvreux, and J. Lafore, 2013: West African monsoon intraseasonal variability: A precipitable water perspective. *J. Atmos. Sci.*, **70**, 1035–1052, doi:10.1175/JAS-D-12-087.1.
- , J.-P. Lafore, R. Roehrig, and F. Couvreux, 2015: Internal processes within the African Easterly Wave system. *Quart. J. Roy. Meteor. Soc.*, **141**, 1121–1136, doi:10.1002/qj.2420.
- Pytharoulis, I., and C. Thorncroft, 1999: The low-level structure of African easterly waves in 1995. *Mon. Wea. Rev.*, **127**, 2266–2280, doi:10.1175/1520-0493(1999)127<2266:TLLSOA>2.0.CO;2.
- Reed, R. J., D. C. Norquist, and E. E. Recker, 1977: The structure and properties of African wave disturbances as observed during phase III of GATE. *Mon. Wea. Rev.*, **105**, 317–333, doi:10.1175/1520-0493(1977)105<0317:TSAPOA>2.0.CO;2.
- , E. Klinker, and A. Hollingsworth, 1988: The structure and characteristics of African easterly wave disturbances as determined from the ECMWF operational analysis/forecast system. *Meteor. Atmos. Phys.*, **38**, 22–33, doi:10.1007/BF01029944.
- Thorncroft, C. D., and M. Blackburn, 1999: Maintenance of the African easterly jet. *Quart. J. Roy. Meteor. Soc.*, **125**, 763–786.
- , and K. Hodges, 2001: African easterly wave variability and its relationship to Atlantic tropical cyclone activity. *J. Climate*, **14**, 1166–1179, doi:10.1175/1520-0442(2001)014<1166:AEWVAI>2.0.CO;2.
- , and B. J. Hoskins, 1994: An idealized study of African easterly waves. I: A linear view. *Quart. J. Roy. Meteor. Soc.*, **120**, 953–982, doi:10.1002/qj.49712051809.
- Vizy, E. K., and K. H. Cook, 2009: Tropical storm development from African easterly waves in the eastern Atlantic: A comparison of two successive waves using a regional model as part of NASA AMMA 2006. *J. Atmos. Sci.*, **66**, 3313–3334, doi:10.1175/2009JAS3064.1.